Journal of
Computational and Theoretical Nanoscience
Vol. 3, 551–559, 2006

Influence of the Metal Contact Size on the Electron Dynamics and Transport Inside the Semiconductor Heterostructure Nanowire

Nenad Radulovic[1], Morten Willatzen[1,*], Roderick V. N. Melnik[1,2], and Lok C. Lew Yan Voon[3]

[1] *Mads Clausen Institute for Product Innovation, University of Southern Denmark, Denmark*
[2] *CRC in Mathematical Modeling, Wilfrid Laurier University, Waterloo, ON, Canada*
[3] *Physics Department, Wright State University, Dayton, OH, USA*

RESEARCH ARTICLE

In this paper, modeling of the transport phenomena inside a nanowire is the central issue. In particular, we present numerical results for a GaAs/AlGaAs semiconductor heterostructure nanowire obtained by a 2D numerical simulation based on a transient quantum drift-diffusion model. The model itself is based on the density-gradient theory proposed by Ancona et al. Due to considering angular-symmetric solutions only, two cylindrical coordinates (r and z) suffice for the investigation. Two different numerical implementations of the model employing the finite difference method and finite element method have been used. Influence of the metal contact size on the carrier dynamics and transport inside the nanowire has been investigated. Current-Voltage (I-V) characteristics for the same heterostructure nanowire supplemented with different combinations of the metal contacts of different sizes are presented and discussed. It has been demonstrated that the size of the metal contacts strongly influences the carrier dynamics and I-V characteristics of the heterostructure nanowire and that it is possible to produce and tune N-shape of the I-V characteristics by changing the size of the metal contacts. This is of interest in relation to optimization of I-V characteristics of resonant tunneling nanostructures.

Keywords: Semiconductor Heterostructure Nanowire, Resonant Tunneling, Metal Contacts.

1. INTRODUCTION

The concept of semiconductor heterostructure nanodevices and their implementation into advanced electronic and photonic systems has led to strong technological conquests and impacts on the commercial market are expected.[1] The idea of semiconductor heterostructure devices may be described as a controlled construction of the potential landscape by appropriately designed combination of layers made of different (semiconductor) materials with different bandgaps.[2]

In this work, the main idea is to numerically investigate the transport phenomena inside a semiconductor heterostructure nanowire. We employ a transient quantum drift-diffusion model to study the influence of the metal contact size on the electron dynamics and transport phenomena inside a GaAs/AlGaAs semiconductor heterostructure nanowire in 2D. Due to the consideration of the axis-symmetrical solutions only, two cylindrical coordinates r and z suffice for the analyses. Effects due to the charge carriers, geometry, and quantum aspects are accounted for in a computationally effective way as compared to the usual full quantum-mechanically based models which become extremely complex in 2D and 3D.

The paper is organized as follows. The transient quantum drift-diffusion model is presented in Subsection 2.1. Geometry of the heterostructure nanowire and different combinations of the metal contacts are displayed in Subsection 2.2. Initial and boundary conditions are highlighted and discussed in Subsections 2.3 and 2.4, respectively. The finite difference and finite element methods, which have been employed for numerical simulations, are illuminated in Subsection 2.5. Geometry and physical parameters of the nanowire are indicated in Subsection 3.1. The time step and spatial mesh are commented on in Subsection 3.2. The convergence of the numerical results and positivity of the electron density are examined in Subsection 3.3. Obtained numerical results are presented and discussed in Subsection 3.4. The summary and the main conclusions are finally given in Section 4.

*Author to whom correspondence should be addressed.

 1546-198X/2006/3/551/009 doi:10.1166/jctn.2006.010

2. THEORY AND NUMERICAL SIMULATION

2.1. Transient Quantum Drift-Diffusion Model

It is well known that the classical drift-diffusion model has been obtained by assuming that internal energy densities of the electron and hole gases have a logarithmic dependence on the corresponding charge densities.[3–5] A more general series expansion of the density using kinetic theory of gases shows that the energy depends not only on the carrier density but also on the gradient of the density, especially when the latter is expected to be non-negligible or even significant which is a typical case in ultra-small semiconductor heterostructures.[6,7]

In this paper, we use a transient quantum drift-diffusion model (TQDDM).[8,9] The model is a set of macroscopic equations and is based on so-called density-gradient theory, which involves the lowest-order quantum correction in the classical drift-diffusion description of the carrier transport in semiconductor nanodevices due to the inclusion of the density-gradient term.[10] The main idea of the density-gradient theory (DGT) proposed by Ancona et al.,[6,7] is that a more general equation of state for the electron gas (the relation between the stress tensor and the electron density), which contains dependence on the electron density as well as on the gradient of the electron density, should be able to describe "behavior" of the electrons in ultra-small semiconductor devices where classical drift-diffusion model cannot be used for accurate investigations.[10] The quantum correction allows the model to account for the lowest order quantum-mechanical effects, i.e., to account for the quantum confinement inside the quantum wells and resonant tunneling through the potential barriers. It has been already shown that the generalized carrier-transport equation accurately describes some of the important quantum-mechanical phenomena including quantum confinement effects and resonant tunneling, see e.g. Refs. [6, 7, 10].

The transient quantum drift-diffusion model can be expressed as a coupled system of scaled governing PDEs and scaled Poisson Equation.[9,11,12]

$$\frac{\partial n}{\partial t} = div(n\nabla F) \tag{1a}$$

$$-\varepsilon^2 \frac{\Delta\sqrt{n}}{\sqrt{n}} + \log(n) + (V + V_B) = F \tag{1b}$$

$$-\lambda^2 \Delta V = (n - C) \tag{1c}$$

where the unknowns are the electron density n, the (quantum) quasi-Fermi level F, and the electrostatic potential V. The barrier potential (see Subsection 2.2) is denoted as V_B, while ε and λ are the scaled Planck constant and scaled Debye length, respectively. The time-independent doping profile C represents distribution of charged background ions. Expressions for the scaled Planck constant ε, scaled Debye length λ, and scaled relaxation time τ_0 are[9,11,12]

$$\varepsilon^2 = \frac{\hbar^2}{6mk_B T_0 L^2}, \quad \lambda^2 = \frac{\varepsilon_s k_B T_0}{q^2 C_m L^2}, \quad \tau_0^2 = \frac{k_B T_0 \tau^2}{mL^2} \tag{2a,b,c}$$

The physical constants are the elementary charge q, the Boltzmann constant k_B, the electron effective mass m, and the reduced Planck constant $\hbar$. The physical parameters are the semiconductor permittivity ε_s, the device operating temperature T_0, and the maximum of the doping profile C_m, while L is the length of the device.

2.2. Geometry of Heterostructure Nanowire

The axial cross section of the semiconductor heterostructure nanowire is presented in Figure 1. The cylindrical coordinates r and z, geometry parameters of interest, i.e., the radius R and length L of the nanowire are clearly indicated, as well as the position and radius of the metal contacts R_{MC}. It is assumed that the nanowire consists of only three homogeneous layers, a GaAs quantum well which is sandwiched between two AlGaAs barriers. The layers are perpendicular to the main axis of the nanowire forming a resonant tunneling semiconductor heterostructure. It is important to note that, due to the assumed axial symmetry of the nanowire and axis-symmetrical metal contacts, only the upper half-part of the cross section of the nanowire represents 2D domain Ω in all numerical simulations presented in this work.

The 2D domain Ω for numerical simulations is reduced to upper half part of the axial cross section of the nanowire. The domain Ω is defined as Ω: $\{r \in (0, R);\ z \in (0, L)\}$, where R is the radius and L is the length of the nanowire. The boundaries $\partial\Omega$ have two disjoint parts: the metal contacts, i.e., Γ_D: $\{r \in [0, R];\ z = 0, L\}$, and insulating (semiconductor) parts of the nanowire, i.e., the main axis and surface of the nanowire, Γ_N: $\{r = 0, R;\ z = (0, L)\}$. It is important to note that $\Gamma_D \cup \Gamma_N = \partial\Omega$ and that $\Gamma_D \cap \Gamma_N = \emptyset$ (see e.g. Ref. [13]).

In Figures 2–3, geometries of the metal contacts for six different cases under consideration in this paper are displayed. In the case when the metal contacts are not of

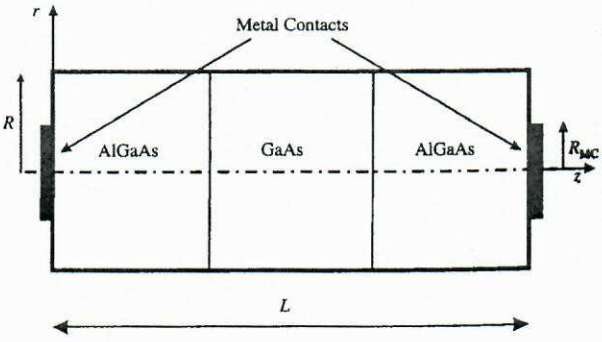

Fig. 1. The axial cross section of the semiconductor heterostructure nanowire. The cylindrical coordinates, r and z, radius R and length L of the nanowire, positions of the metal contacts and their radius R_{MC} are clearly indicated. Presented heterostructure nanowire consists of only three homogeneous layers, a GaAs quantum well sandwiched between two AlGaAs barriers, which are perpendicular to the nanowire axis. The upper half-part of the axial cross section represents 2D domain Ω for all numerical simulations presented in this work.

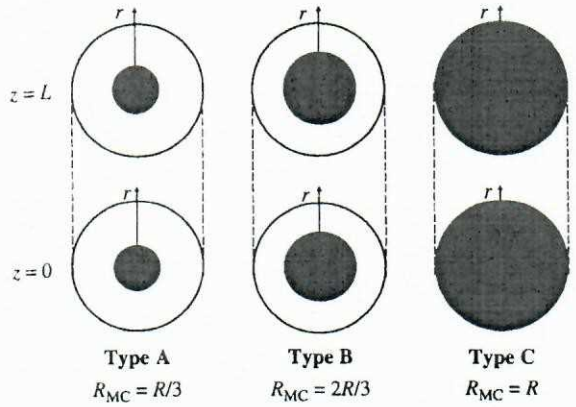

Fig. 2. Three different combinations of the metal contacts of the same sizes. Two cross sections of the nanowire, at positions $z = 0$ and $z = L$, for three nanowires with different sizes of the metal contacts R_{MC} are shown. For the simplicity, they are denoted as type A, B, and C. The corresponding sizes of the metal contacts are: $R_{MC} = R/3$, $R_{MC} = 2R/3$, and $R_{MC} = R$, respectively. Note: In this case, the sizes of the metal contacts at both ends of the nanowire are the same, and they are measured starting from the main axis of the nanowire.

the full size, i.e., when $R_{MC} < R$, the domain Ω stays unchanged while the boundaries are affected. The boundaries regarding the metal contacts are now reduced and they are defined as Γ_D: $\{r \in [0, R_{MC}]; z = 0, L\}$, while the boundaries regarding semiconductor parts of the nanowire are extended for the part which is not covered with the metal contacts, i.e., for Γ_N: $\{r \in [R_{MC}, R]; z = 0, L\}$.

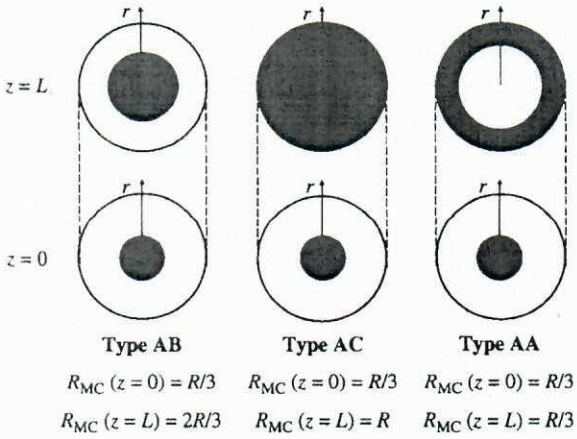

Fig. 3. Three different combinations of the metal contacts of different sizes. Two cross sections of the nanowire, at positions $z = 0$ and $z = L$, for three nanowires with different combinations of the metal contacts of different sizes R_{MC} are shown. For the simplicity, they are denoted as type AB, AC, and AA. The corresponding sizes of the metal contacts are: R_{MC} $(z = 0) = R/3$ and R_{MC} $(z = L) = 2R/3$; R_{MC} $(z = 0) = R/3$, and R_{MC} $(z = L) = R$; and R_{MC} $(z = 0) = R/3$ and R_{MC} $(z = L) = R/3$; respectively. Note: In this case, the sizes of the metal contacts at the ends of the nanowire are not the same. Also, in the case of type AA metal contacts, the size of the metal contact R_{MC} $(z = L) = R/3$ is measured in opposite direction, i.e., from the surface $(r = R)$ towards the nanowire axis $(r = 0)$.

2.3. Initial Conditions

The system of Eqs. (1) must be supplemented with appropriate initial and boundary conditions. It is natural to employ the following initial conditions[9, 11, 12] in the domain of interest Ω. The electron density n is chosen to be equal to the doping profile C, while the initial conditions for the quasi-Fermi level F and electrostatic potential V, in thermal equilibrium (no bias), are chosen to be zero. Hence, the initial conditions we have used are

$$n(t=0) = n_0 = C, \quad F(t=0) = F_0 = 0, \quad V(t=0) = V_0 = 0 \tag{3a,b,c}$$

Note that the initial conditions in thermal equilibrium are indicated with a subscript 0. These initial conditions represent a natural choice (in thermal equilibrium) which is physically motivated, and they are frequently used in computer simulations of semiconductor devices.[3–5] The first expression, which defines initial condition for the electron density, is based on the assumption that total ionization inside the semiconductor device is present (i.e., that all donor and acceptor atoms are ionized). The second initial condition, for the quasi-Fermi level, is based on the requirement that the current density in thermal equilibrium ($V_{BIAS} = 0$) is equal to zero ($J = -n\nabla F \equiv 0 \Rightarrow F =$ const.). The initial condition for the electrostatic potential is electrostatically motivated ($V_{BIAS} = 0 \Rightarrow J \equiv 0 \Rightarrow V =$ const. $= 0$).

If the doping profile is not constant (e.g., different parts of the semiconductor device are being of different type) or if we are dealing with a heterostructure, it is physically correct and natural to expect that $n_{eq} \neq C$, $F_{eq} =$ const, and $V_{eq} \neq 0$ (where indexes eq denote thermal equilibrium values, i.e., results or values which are obtained when $V_{BIAS} = 0$). Inside a heterostructure in thermal equilibrium ($V_{BIAS} = 0$), it is natural and physically motivated to expect that there will be an accumulation of the electrons in the quantum well and a lack of the electrons in the barriers resulting in $n_{eq} \neq C$. As a consequence, so-called built-in electrostatic potential will rise inside such semiconductor device. This potential is responsible for keeping a balance between diffusion of the charge carriers and resulting electrostatic field in the state of thermal equilibrium resulting in $V_{eq} \neq 0$ and $J_{eq} \equiv 0$. On the other hand, it is required that the current density in thermal equilibrium ($V_{BIAS} = 0$) should be identically equal to zero, i.e., $J_{eq} \equiv 0$, due to the laws of the electrostatics. Hence, the quasi-Fermi level inside the device in thermal equilibrium should be constant, which follows from Eq. (1a), and from the expression for the current density ($J = -n\nabla F$) and this constant should be zero, i.e., $F_{eq} \equiv 0$, due to the boundary conditions ($F \equiv 0$ at the boundaries when $V_{BIAS} = 0$).

Regarding the initial conditions when $V_{BIAS} \neq 0$, it is usual to employ numerical results for the electron density, quasi-Fermi level, and electrostatic potential obtained in

the equilibrium case, i.e., n_{eq}, F_{eq}, and V_{eq}, respectively, as initial conditions for the calculations when a small bias is applied ($V_{BIAS} \sim 10$ mV). In general, it is usual to employ numerical results which have been obtained for the previous value of the applied bias as initial conditions for the next (higher) applied bias. Doing that, one will avoid potential numerical problems (divergence of numerical results) and certainly speed up the calculations (faster convergence due to the better initial guess). Also, for the reason to avoid potential numerical instabilities, the bias step should be small enough, and at the same time, big enough to avoid expensive calculations of the I-V characteristic of the semiconductor heterostructure (i.e., to reduce the total number of I-V points). We have found that the bias step of 10 mV satisfies both requirements and we have used this bias step in all calculations presented in this work.

2.4. Boundary Conditions

The boundary conditions which have been implemented at the boundaries $\partial\Omega$ are physically motivated and commonly employed in the modeling of the semiconductor nanostructures, see e.g., Refs. [8, 9, 11]. The boundary $\partial\Omega$ consists of two disjoint parts (see Subsection 2.2) which are usually denoted with Γ_D and Γ_N representing the parts of the boundary where the Dirichlet and Neumann boundary conditions should be applied, respectively. Regarding the boundary conditions, it is convenient to assume for the electron density to fulfill local charge neutrality at the metal contacts, if the device is not too small (e.g., if $L >$ 10 nm). Further, it is natural to assume that there is no normal component of the total current density (including the quantum current density) along the insulating part of the boundary. Finally, we assumed that no quantum effects occur at the metal contacts. These boundary conditions are physically motivated and commonly employed in the quantum-corrected macroscopic modeling of semiconductor devices, see e.g., Refs. [9, 11, 12, 14].

Usually, it is assumed that the metal contacts are ideal conductors (being infinite reservoirs of the electrons). Thus, the metal contacts can be modeled using the Dirichlet boundary conditions[9, 11, 12, 14]

$$n = n_D, \quad F = F_{eq} + V_{BIAS}, \quad V = V_{eq} + V_{BIAS}, \quad \text{on } \Gamma_D \tag{4a,b,c}$$

where n_D is equal to the doping of the semiconductor material (i.e., $n_D = C_{max}$), F_{eq} is equilibrium value of the quasi-Fermi level (recall $F_{eq} = 0$), and V_{eq} is the equilibrium value of the electrostatic potential (so-called built-in electrostatic potential, in general $V_{eq} \neq 0$).

At the same time, it is usual to model the insulating part of the nanodevice employing the Neumann boundary conditions[9, 11, 12, 14]

$$\nabla n \cdot \upsilon = 0, \quad \nabla F \cdot \upsilon = 0, \quad \nabla V \cdot \upsilon = 0, \quad J \cdot \upsilon = 0, \quad \text{on } \Gamma_N \tag{5a,b,c}$$

where υ is the unit outward normal vector along Γ_N. The Neumann boundary conditions are based on the assumption that there is no normal component of the total current density across the boundaries which represent insulating (i.e., semiconductor) parts of the device. Hence, it is assumed that the current density is localized inside the device and flows through the metal contacts only (with respect to the boundaries of the device). It is important to note that this set of the boundary conditions is motivated by their analogy to the boundary conditions commonly used for the classical drift-diffusion model. A rigorous derivation of the boundary conditions from microscopic quantum-mechanical models, especially for nonequilibrium problems, i.e., when the bias is applied ($V_{BIAS} \neq 0$), is hard to find/perform.[11] Therefore, it is usual to employ semi-classical conditions at the boundaries. However, this is possible only if the characteristic length of the device L is not too small (i.e., when L is in the range of tens of nanometers).[11] For ultra small semiconductor devices, i.e., in so-called quantum limit ($L \to 0$), the classical assumption of the charge neutrality at the boundaries becomes invalid[5] while quantum-mechanical effects can play a significant role.[11]

The current density, which is given by the following expression[8]

$$J = -n\nabla F \tag{6}$$

is localized inside the nanowire, and there is no radial component of the current and electrostatic field close to the outer boundary (i.e., to the surface of the nanowire). This means that near the outer boundary, there should be no changes in the electron density, quasi-Fermi level, and electrostatic potential in the radial direction. Thus, the Neumann boundary conditions for the electron density, quasi-Fermi level, and electrostatic potential are physically motivated and natural choices at the outer boundary of the nanowire.

2.5. Finite Difference and Finite Element Implementations

In this work, we have employed two different numerical implementations of the model. The first implementation has been done using the finite difference method (FDM). The system (1) has been discretized in time and space using the implicit backward Euler method with variable time step, and the finite difference method on the uniform spatial grid in 2D, respectively. The spatial grid is characterized with the following parameters: $\Delta_r = R/M_r$ and $\Delta_z = L/M_z$, ($\Delta_r = \Delta_z = 0.25$ nm), where R is the radius and L is the characteristic length of the nanowire, while $M_r + 1$ and $M_z + 1$ are the total numbers of grid points in r and z directions, respectively. This numerical implementation has been carried out in Matlab using the source code which has been developed as an extension of our source code for 1D case.

The system of algebraic equations, which follows from the system (1) after discretization, has been solved using the Newton iteration procedure[4] at each time step. In all performed calculations in the case of the FDM numerical implementation, no decoupling algorithms have been used, and the results have been obtained simultaneously in each time step for the whole 2D space domain and for all three unknowns n, F, and V. This approach is usually called "brute-force approach" (it is computationally very expensive one).

The second numerical implementation of the model has been done using the finite element method (FEM). The main reason was to speed up the calculations and to perform a validation check of the "flat results" (see Section 3). In this case, the 2D domain has been divided into a big number (approx. 15000) of finite elements (triangles or triangles-like), which gives six times bigger number of degrees of freedom (approx. 90000). Note that the node points are at the corners and at the side midpoints of all mesh triangles. A time-dependent nonlinear solver has been employed for the transient study, while a nonlinear iterative solver has been employed for the steady state simulations. However, in this paper we do not consider the transient regime, only the stationary regime. Hence, a nonlinear iterative solver has been used in all performed computations for all I-V characteristics which are presented in Section 3. This numerical implementation has been carried out in Femlab.

The stopping criterion which has been used inside the Newton iteration procedure in the FDM implementation, is the same one as in 1D case (see Ref. [15]). In 1D case, we use an absolute tolerance $TOL = 10^{-6}$, while in 2D case the accuracy has been reduced, i.e., TOL has been increased to $TOL = 10^{-4}$. Even with a significant increase of the absolute tolerance, the number of the iterations inside the Newton iteration procedure in 2D case is measured in order of tens, while in 1D case the usual number of the iterations is less or equal to 5 (with $TOL = 10^{-6}$, see Ref. [15]). For the comparison, in the FEM implementation, the relative tolerance has been set to $RELTOL = 10^{-3}$ in all performed calculations.

3. NUMERICAL RESULTS

3.1. Geometry and Physical Parameters of Heterostructure Nanowire

In the present paper, the semiconductor heterostructure nanowire under consideration consists of a quantum well (a GaAs layer) sandwiched between two barriers (two AlGaAs layers). Each of the layers is 5 nm thick which result in total length of the nanowire $L = 15$ nm. The nanowire is supplemented with two (ideal) metal contacts at the ends. The radius of the nanowire is $R = 15$ nm, and the barrier potential is assumed to be $V_B = 0.4$ eV. The nanowire is n^+-type, with a constant doping profile $C = 10^{24}\ \mathrm{m}^{-3}$, and all layers are homogeneous which lead to the assumption of axial symmetry of the nanowire. The operating temperature of the nanowire is $T_0 = 77$ K, the effective electron mass is assumed to be $m = 0.067\ m_0$, where m_0 is the electron rest mass, and the permittivity of the nanowire is assumed to be $\varepsilon_s = 13.1\varepsilon_0$, where ε_0 is the permittivity in the vacuum. The electron momentum relaxation time, which is necessary for the numerical simulation in the FDM implementation and for the rescaling of the current density in both implementations, is assumed to be $\tau = 10^{-13}$ s, which is a reasonable value, see e.g., Refs. [9, 11, 12] Recall that one of the main requirements for the scaled relaxation time, Eq. (3c), is that it should be small in comparison to unity due to the zero-relaxation time approximation which has been used during the derivation of the transient quantum drift-diffusion model from the quantum hydrodynamic model (see e.g., Refs. [9, 11, 12]).

3.2. Time Step and Spatial Mesh

In the FDM implementation, the scaled time step which has been initially set to $\tau_0 = 10^{-4}$ (no units) has been increased in order to speed up numerical calculations. On the contrary, a uniform spatial grid for the space discretization with 4 points per nm (ppnm) has been used in all performed calculations in the FDM implementation (hence, $\Delta_r = \Delta_z = 0.25$ nm).

In the FEM implementation, the 2D domain has been divided into approximately 15000 finite elements (triangles), which give almost 90000 degrees of freedom. This mesh ensures that the relative difference between the currents through the opposite metal contacts, i.e., $I(z = 0)/I(z = L)$, is less than 5% (which we consider acceptable for a qualitative study we are interested in).

3.3. Convergence of Numerical Results and Positivity of Electron Density

It has been observed that both implemented methods (FDM and FEM) suffer from the convergence problems if a stationary nonlinear solver is used instead of a time-dependent one, and that the FDM implementation is more sensitive considering the type of the solver. Unfortunately, changing the scaled time step one cannot eliminate the convergence problem in the FDM implementation. Similarly, increasing the spatial resolution one can slow down the calculations and rapidly increase the request for the memory resources, however, it has been observed that this will not improve the convergence of numerical results. Note that the memory is the main problem for numerical simulations based on the FDM implementation.

In 1D case, it has been proved (see e.g. Refs. [9, 12]) that the positivity of the electron density is preserved while, at the same time, it has been pointed out that it is not easy to prove the positivity in dimensions higher than

one. To the best of our knowledge, an exact proof of the positivity in dimensions higher than one has not been published yet. Therefore, we have monitored positivity of the electron density and in all performed calculations in 2D, for different nanowires and for both implemented methods (FDM and FEM), preservation of the positivity for the electron density has been perceived.

3.4. Numerical Results and Discussion

Dimensions of the semiconductor heterostructure nanowire under consideration ($R = 15$ nm, and $L = 15$ nm) give us a good reason to expect interesting phenomena where quantum mechanical effects are heavily involved. The reason for "choosing" the nanowire of that size is a practical one, i.e., the idea was to compare numerical results obtained with two different implementations (FDM and FEM) of the transient quantum drift-diffusion model in 2D. Recall that the 2D numerical simulations are memory consuming (especially our FDM implementation, as mentioned in Section 2), which heavily influenced on the "choice" of the size of the nanowire under consideration.

We are aware of the fact that the numerical results obtained in this work can be used for a qualitative study only. Hence, unexpected phenomena which have been observed, i.e., a strong influence of the size of the metal contacts on the electron dynamics, transport, and consequently on the I-V characteristic of the nanowire, could be a good starting point for a full quantum-mechanical approach in 2D, and/or for some experimental studies in the future.

One of the first conclusions regarding obtained numerical results in 2D was that the results do not show any radial dependency ("flat results") when the Neumann boundary conditions have been employed at the outer boundary of the nanowire, if the nanowire is supplemented with the full size metal contacts, i.e., $R_{MC}(z = 0) = R_{MC}(z = L) = R$. This means that the 2D problem can be reduced to the 1D problem under the given conditions. From the physical point of view, one can understand that there is no explicit radial dependence (homogeneous layers of the semiconductor heterostructure nanowire, axis-symmetrical full size metal contacts, and constant doping), and that could be the reason for the "flat results."

However, it has been observed that if the metal contacts are reduced to 1/3 or 2/3 of the full size, i.e., $R_{MC} = R/3$ or $R_{MC} = 2R/3$, respectively, the numerical results show a strong radial dependence. Thus, the following study of the GaAs/AlGaAs nanowires with $R = 15$ nm and $L = 15$ nm is based on the different sizes of the metal contacts, i.e., the influence of the size of the metal contacts on the electron dynamics, transport, and on the I-V characteristic of the nanowire has been investigated.

Obtained numerical results for the normalized electron density in the central GaAs layer of the nanowire under consideration are given in Table I. The first row shows the applied bias which is expressed in [V], while the second row shows the position along the radial direction, i.e., the nanowire axis ($r = 0$) and its surface ($r = R$), where the maxima of the electron density have been recorded. The maxima of the electron density in the longitudinal direction have been reached in the middle of the central layer ($z = L/2$) in thermal equilibrium (no bias), and a small shift of the maxima in the $z = 0$ direction (i.e., towards grounded metal contact) has been observed when the bias is applied. In the following rows in Table I, the maxima of the electron density (normalized to C, where C is the doping of the nanowire) inside the central layer of the nanowire supplemented with the metal contacts of different sizes and with different combinations of the metal contacts of different sizes are given. For the types of the metal contacts, see Figures 2–3 in Subsection 2.2. Note that if the metal contacts are of the same size, they are denoted with one letter (A, B, and C), and if the metal contacts are of different sizes they are denoted with two letters (AB, AC, and AA).

From Table I, one can see that for zero bias and for smaller size metal contacts the maximum of the electron density, which is reached at the surface of the nanowire, is much higher than for the full-size metal contacts. In addition, the difference between the electron density at the axis and at the surface of the nanowire is higher for smaller metal contacts, while there is no difference between them for the metal contacts of the full size (so-called "flat results," i.e., the results do not show radial dependence at all). For different combinations of the metal contacts of different sizes, the electron density is (again) higher at the surface of the nanowire while the difference between the electron density at the axis and at the surface of the nanowire is smaller in comparison with the corresponding one for the metal contacts of the same size. Apart from that, it has been observed that the electron

Table I. The maxima of normalized electron density in the middle of the central layer of the nanowire.

	$V_{BIAS} = 0.00$	$V_{BIAS} = 0.00$	$V_{BIAS} = 0.25$	$V_{BIAS} = 0.25$	$V_{BIAS} = 0.50$	$V_{BIAS} = 0.50$
	$r = 0$	$r = R$	$r = 0$	$r = R$	$r = 0$	$r = R$
A	1.9044	4.4100	1.7161	4.3264	1.5876	4.0401
B	0.6084	1.7424	0.1849	0.8464	0.0400	0.2025
C	0.2304	0.2304	0.0169	0.0169	0.0036	0.0036
AB	1.2100	3.0625	2.1025	2.5600	1.2769	0.9604
AC	1.0404	1.9600	2.7225	1.3689	0.3600	0.0144
AA	2.1316	2.2500	3.6100	0.8464	0.0841	0.0004

have a tendency to accumulate in the part of the central layer which is not "covered" with the metal contacts.

At the same time, from Table I follows that the influence of the applied bias on the electron dynamics inside the central layer of the nanowire under consideration is different for different types of the metal contacts. One can clearly see that for the same size metal contacts, the influence of the applied bias on the electron density increases with the increase of the size of the metal contacts. In this case, an increase of the bias produces a decrease of the electron density. Similarly, for different combinations of the metal contacts of different sizes, a bigger difference between the sizes of the metal contacts produces a stronger influence of the applied bias on the electron density. In this case, the increase of the bias influences on the electron density at the axis and at the surface of the nanowire in different ways. At the axis, the electron density firstly increases and then decreases with the increase of the bias, while at the surface the increase of the bias produces decrease of the electron density.

In addition, it has been observed that for the semiconductor heterostructure nanowire with the metal contacts of the same size (type A, B, and C), the increase of the bias produces decrease of the electron density in the central GaAs layer. The influence of the bias on the electron density is proportional to the size of the metal contacts, i.e., the bigger the size—the stronger the influence. Decrease of the electron density is present at both positions of the interest, i.e., at the axis, and at the surface of the nanowire. At the same time, the influence of the applied bias stay unchanged, increases, or decreases with the increase of the applied bias, depending on the size of the metal contacts.

On the contrary, it has been observed that the bias influences in different ways on the electron density in the central GaAs layer at the axis and at the surface when the nanowire is supplemented with different combinations of the metal contacts of different sizes (type AB, AC, and AA). At the axis of the nanowire, the electron density firstly increases and then decreases with the increase of the bias, while at the surface of the nanowire the electron density decreases with the increase of the bias. On the contrary to the same-size metal contacts case, the influence of the bias on the electron density now increases with the increase of the bias and it is more pronounced for a bigger difference between the sizes of the metal contacts. It has been observed that the influence of the applied bias on the electron density is the strongest one when the nanowire is supplemented with AA type of the metal contacts.

In short, one can conclude that the electron dynamics inside the central layer of the semiconductor heterostructure nanowire under consideration strongly depend on the size and on the difference in the sizes of the metal contacts (the nanowire is supplemented with). It is important to note that in the case of the nanowire with the metal contacts of different sizes, the electrons in the central GaAs layer at or near the axis show a similar "behavior" as the electrons in the resonant tunneling devices which have N-shape I-V characteristics. First, with the increase of the bias, the electrons accumulate inside the central layer, and afterwards, with a further increase of the bias, they show a tendency to escape from the central layer. This means that with an appropriate combination of the metal contacts of different sizes one can artificially force the electrons to accumulate inside the central layer (when the applied bias is small, i.e., $V_{\mathrm{BIAS}} \leq 250$ mV for this particular case). At the same time, as a direct consequence of this "artificial manipulation" with the electrons, one can certainly influence on the electric response of the nanowire as well. Hence, one would expect that it is possible to produce (quasi) N-shape I-V characteristic of the nanowire in an "artificial way," i.e., with an appropriate combination of the metal contacts of different sizes even if the semiconductor heterostructure nanowire is constantly doped.

To demonstrate different influences of the applied bias on the electrons inside the central layer of the nanowire, the electron densities inside the semiconductor heterostructure nanowire under consideration, supplemented with the metal contacts of the same size (A type, left graphs) and with the metal contacts of different sizes (AB type, right graphs), are given in Figure 4. The top graphs show the electron density in thermal equilibrium (no bias) and the bottom graphs show the electron density for the applied bias equal to 0.5 V.

From Figure 4, one can clearly see that the influence of the applied bias on the electron density inside the nanowire is significantly different in the case when the nanowire is supplemented with the metal contacts of the same size and with a combination of the metal contacts of different sizes. In particular, the electron density stays almost unchanged when the nanowire is supplemented with A type of the metal contacts and become completely different when the nanowire is supplemented with AB type of the metal contacts.

The total current through the nanowire is calculated using the following expression due to the (assumed) axial symmetry of the nanowire and axis-symmetric metal contacts

$$I = 2\pi \int_0^{R_{\mathrm{MC}}} J(r) r \, dr \tag{7}$$

The corresponding I-V characteristics of the (same) heterostructure nanowire under consideration supplemented with the metal contacts of the same size, i.e., A, B, and C type of the metal contacts (left graph), and supplemented with different combinations of the metal contacts of different sizes, i.e., AB, AC, and AA type of the metal contacts (right graph), are shown in Figure 5.

From the graphs in Figure 5, one can clearly see that different influences of the applied bias on the electron density inside the same heterostructure nanowire, supplemented with the metal contacts of different sizes (left graph) and

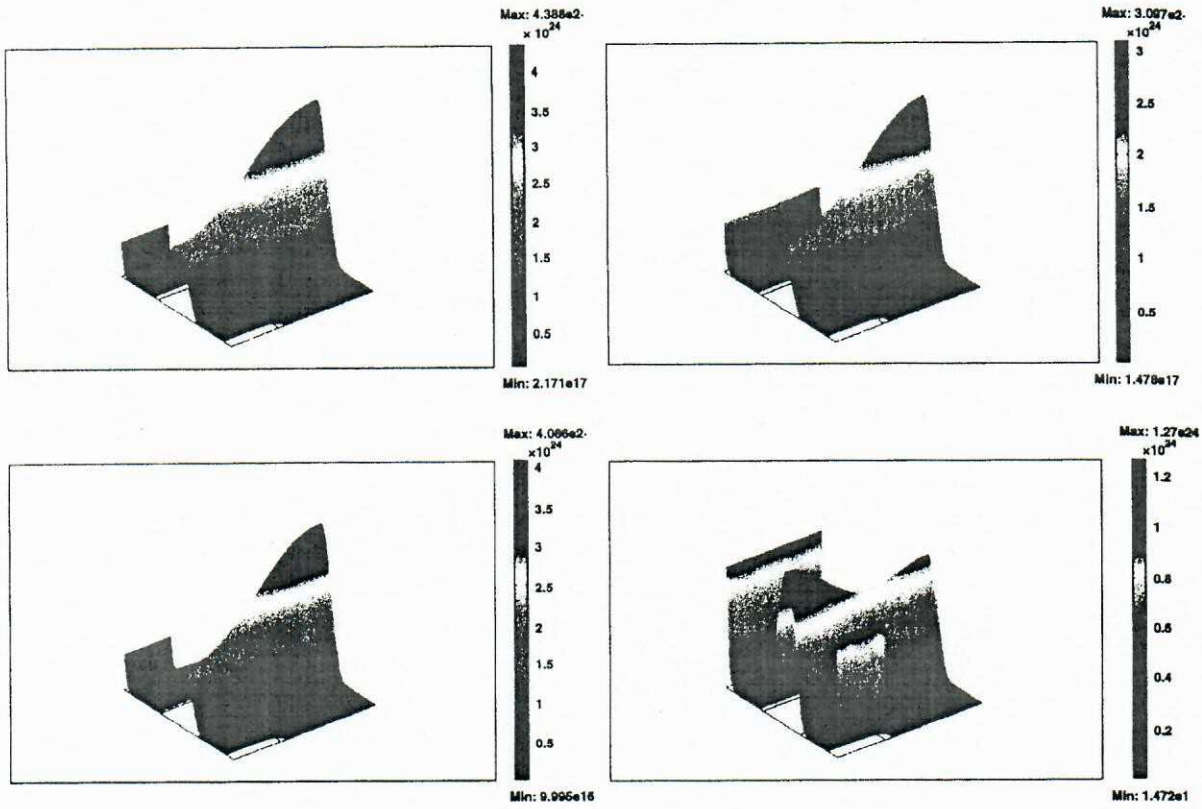

Fig. 4. The electron density in thermal equilibrium, i.e., no bias (top graphs), and for $V_{BIAS} = 0.5$ V (bottom graphs), inside the GaAs/AlGa nanowire with metal contacts of the same size (type A, left graphs), and with metal contacts of different sizes (type AB, right graphs). For the ty of metal contacts, see Figures 2–3 in Subsection 2.2.

with different combinations of the metal contacts of different sizes (right graph), result in completely different electric responses of the nanowire, i.e., in completely different I-V characteristics. In short, one can conclude that the size of the metal contacts significantly influence on the electron dynamics and consequently on the I-V characteristic of the (same) semiconductor heterostructure nanowire. Apart from that, one can conclude that with an appropriate combination of the metal contacts of different sizes, it possible to influence on the I-V characteristic of the he erostructure nanowire, to produce and tune N-shape, a to obtain a bigger peak-to-valley current ratio, even in th case when the semiconductor heterostructure nanowire constantly doped. This could be of interest in the proce of optimization of the I-V characteristics of the resona tunneling heterostructure nanowires and nanostructures.

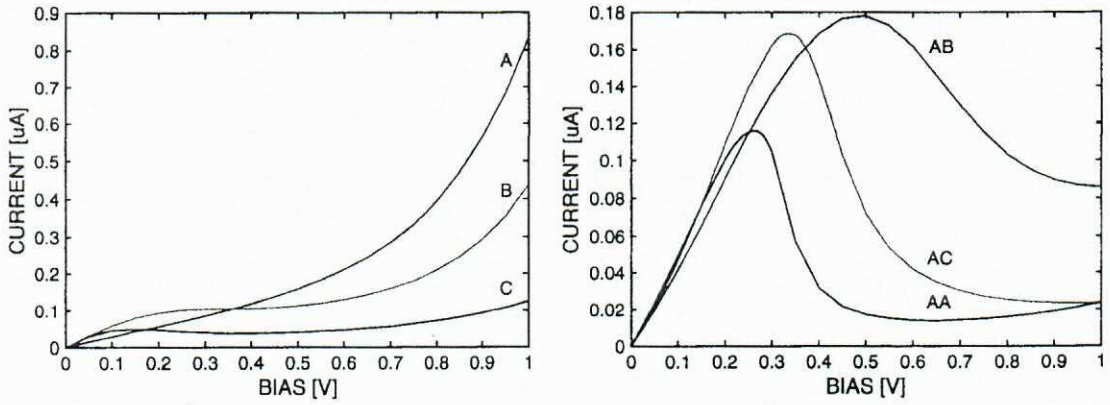

Fig. 5. The I-V characteristics of the same semiconductor heterostructure nanowire supplemented with metal contacts of the same size, i.e., A, B, C type (left graph), and with metal contacts of different sizes, i.e., AB, AC, and AA type (right graph). For the types of metal contacts, see Figures 2 in Subsection 2.2.

SUMMARY AND CONCLUSIONS

n this paper, the transient quantum drift-diffusion model as been employed to simulate transport processes in the emiconductor heterostructure nanowire in 2D. The model as been expressed in cylindrical coordinates, r and z, due o the consideration of the angular-symmetric solutions nly. Two different methods, the FDM and FEM, have een successfully implemented for the numerical simulaions. We have found that the positivity of the electron lensity holds for all examples considered in this work for both implementations). Regarding obtained numerical esults, a strong influence of the size of the metal conacts on the electron dynamics inside the semiconductor eterostructure nanowire has been observed. In addition, it has been observed that with an appropriate combination of the metal contacts of different sizes one can artificially force the electrons to accumulate inside the central layer. Consequently, the size of the metal contacts significantly influences on the transport processes inside the semiconductor heterostructure nanowire and on its electric response. Apart from that, it has been observed that it is possible to produce N-shape I-V characteristic of the semiconductor heterostructure nanowire with an appropriate combination of the metal contacts of different sizes even in the case of the constant doping (of the nanowire), and that it is possible to change peak-to-valley current ratio as well. Hence, we can conclude that one should be able to design/tune the I-V characteristic of the semiconductor heterostructure nanowire by changing the size of the metal contacts, keeping the physical parameters and geometry of the nanowire completely unchanged. This could be useful in the process of optimization of the I-V characteristics of the resonant tunneling nanowires and nanodevices.

References

1. B. Bhushan (ed.), Springer Handbook of Nanotechnology, Springer-Verlag, Berlin (**2004**).
2. J. Orton, The Story of Semiconductors, Oxford University Press, Oxford (**2004**).
3. M. S. Mock, Analysis of Mathematical Models of Semiconductor Devices, Boole Press, Dublin (**1983**).
4. S. Selberherr, Analysis and Simulation of Semiconductor Devices, Springer-Verlag, Wien, New York (**1984**).
5. P. A. Markowich, C. A. Ringhofer, and C. Schmeiser, Semiconductor Equations, Springer-Verlag, Wien (**1990**).
6. M. G. Ancona and H. F. Tiersten, *Phys. Rev. B* 35, 7959 (**1987**).
7. M. G. Ancona and G. J. Iafrate, *Phys. Rev. B* 39, 9536 (**1989**).
8. R. Pinnau and A. Unterreiter, *SIAM J. Numer. Anal.* 37, 211 (**1999**).
9. R. Pinnau, *ZAMM* 80, 327 (**2000**).
10. M. G. Ancona, *Phys. Rev. B* 42, 1222 (**1990**).
11. R. Pinnau, *Appl. Math. Lett.* 12, 77 (**1999**).
12. R. Pinnau, *Nonlin. Anal.* 47, 5849 (**2001**).
13. G. M. Troianiello, Elliptic Differential Equations and Obstacle Problems, Plenum Press, New York (**1987**).
14. A. Jüngel and R. Pinnau, *SIAM J. Num. Anal.* 39, 385 (**2001**).
15. N. Radulovic, M. Willatzen, and R. V. N. Melnik, in Lecture Notes in Computer Science, edited by A. Lagana et al., Berlin, Springer-Verlag (**2004**), Vol. 3045, p. 817.

Received: 30 November 2005. Accepted: 1 March 2006.